

Analysis of the multi-cell correlation of the slow fading from UMTS measurements and its impact on radio network planning

Jürgen Beyer, Linghan Mao
Deutsche Telekom, Bonn, Germany

Abstract — In order to further improve the cell edge throughput prediction for network planning and optimisation purposes the correlation properties of the received power from pairs of cells is investigated. Since the results should match the typical scenarios of UMTS and LTE networks in urban areas we analysed own measurements. A system of the standard drive test equipment is applied enabling to evaluate a comprehensive data set from four cities of different size. Although highly focussing base station antennas are used the received power from intra-site cells is observed to be highly correlated whereas the signals from widely separated base station antennas are clearly uncorrelated. That agrees with other studies and indicates that our proposed measurement set-up and post-process are suited for signal correlation analysis. Considering the outcome of this study in our RF planning tool the cell edge predictions are closer to the experience from throughput measurements.

Keywords — *slow fading correlation, radio network planning, throughput prediction*

I. INTRODUCTION

Current and future mobile radio networks are designed to serve the growing demand of mobile internet access where the traffic in the downlink is significantly higher than in the uplink. Therefore, the downlink is more in the focus of mobile radio network planners and strategic planning departments as the uplink is. For single frequency networks, like UMTS and LTE, the downlink capacity is interference limited and a precise propagation model only is not sufficient for a precise downlink throughput prediction.

In mobile radio network planning we regard higher exceeding percentiles of, e.g., coverage probability or throughput. To compute the higher throughput percentiles in the downlink requires to calculate the distribution of the signal to interference power ratio (SINR). Several random processes, like imperfect power control or different cell transmission power due to varying traffic, affect the SINR distribution but the dominating random effect is the slow fading. In consequence, in particular at the cell edge the SINR distribution depends also on the correlation of the signals from serving and interfering cells. This motivated us to investigate the multi-cell correlation of the slow fading.

The multi-cell correlation of the slow fading is comprehensively covered in the literature. According to [1] the slow

fading of signals from two cells is highly correlated if the angle of arrival differences (AAD; means the angle between the links to both base stations) is small and that the correlation decreases with increasing AAD. For $AAD < 10^\circ$ they observe correlation coefficients on the order of 0.6 to 0.8. A demonstrative model simulating this relationship is presented in [2]. A dependency between the correlation and the AAD is in [3] only observed for closely positioned base station antennas ($\sim 50\text{m}$) but for widely separated antennas ($\sim 900\text{m}$) the slow fading is found to be clearly uncorrelated which is also confirmed by [4]. Based on channel sounder measurements the slow fading of signals from different sites is also observed to be uncorrelated and even the received power from two sectors of one site is only highly correlated for line of sight (LOS) [5].

Many of those studies are based on a quite small data set, the base station antennas are higher and/or the inter-site distances are larger than for UMTS and LTE networks in large and medium-sized cities which might lead to different slow fading correlation properties. Therefore, we carried out the correlation analysis utilising own measurements in the Deutsche Telekom's UMTS network. In order to get a large data set we were looking for a cost and time efficient way to collect comprehensive measurement data and applied a PN scanner which is part of our standard drive test equipment.

In this paper we shortly describe the measurement system and introduce the proposed post-process in Section III. The correlation results observed from drive tests in four cities of different sizes in two countries are presented in Section IV. We concentrate on the power correlation from inter- and from intra-site cells. Finally, the impact of the slow fading correlation on the predicted downlink throughput is shown.

II. MEASUREMENT SYSTEM AND AREAS

The correlation analysis described in this paper is based on PN scanner measurements. Apart others a PN scanner measures the received primary common pilot channel (pCPICH) power of up to 8 cells per measurement point. The power of those cells is measured which are up to 20dB below the highest received power. A similar measurement system is used for LTE too.

A PN scanner is part of the standard drive test equipment of network operators used, e.g. for network optimisation purposes. Therefore, the Deutsche Telekom is permanently performing scanner measurements and this large amount of data is also available for the power correlation analysis. Getting the measurements 'by the way' is one advantage of the analysis procedure suggested in this paper.

Typically, in urban areas the base station antennas are located only few metres above the surrounding roof tops. The sites are equipped with three sectors with a boresight offset of 120 degrees. Most of the UMTS antennas have a quite small vertical beam width of 6 degree.

In this paper we regard measurements from 4 cities in 2 countries: Cologne (Germany, 1 Million inhabitants), Friedrichshafen (Germany, 60,000 inhabitants), Leeuwarden (Netherlands, 95,000 inhabitants) and Drachten (Netherlands, 45,000 inhabitants). Since the measurements cover a wide range of urban development the observed correlation results have a high statistical reliability. For specific analysis the measurements in Cologne are divided into regions with different environments (dense urban, residential). In Cologne, we additionally regard some single streets where LOS is mainly given. The measurements in the other cities are 'normal' drive tests and, thus, they are not further subdivided. All together measurement data along more than 100km is evaluated and the number of involved cells is on the order of 150.

III. THE MEASUREMENT POST-PROCESS

The PN scanner measures the pCPICH power without any averaging. Hence, the measurements contain the fast fading which has to be removed for the correlation analysis. However, due to the relative low rate of 6 samples per second the interval length for averaging has to be longer than usually (please note that the measurements in the Netherlands have higher sample rate since less parameters are detected). After visually checking the outcome of different interval lengths we finally regard an interval length of 20m as a fair trade-off between the number of samples per interval (10 on average) and the interval length. A sliding average is applied providing a local power average (P_{la}) per sample point – means, the

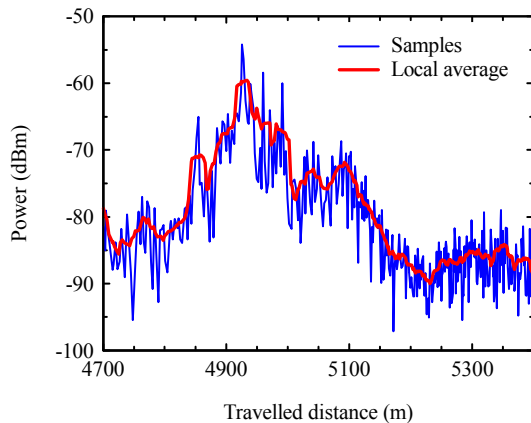


Figure 1: The pCPICH power (samples) measured by the PN scanner and the local power average ($=P_{la}$) given by the sliding average filter for a short route section.

number of power values is the same after averaging. The samples together with the sliding average for a short part of a measurement route are shown in Figure 1.

The sliding average is applied to the received power from all cells within a route interval. But the group of cells simultaneously detected per sample point might change within a route interval. E.g., in the worst case a cell is detected at only one sample point. In order to get a reliable average a cell j is only considered if within a sliding average interval the rule

$$N_{mp,j} \geq N_{mp} - 1 \quad (1)$$

is hold with

- N_{mp} Number of measurement points within the regarded route interval
- $N_{mp,j}$ Number of measurement points where cell j is detected in a route interval.

This strict condition in the sliding average procedure significantly reduces the number of cells per route interval.

Basically, the slow fading correlation of the path loss should be investigated and, therefore, the effect of the base station antenna pattern should be removed. In principle, easy to do, but in practice there are several uncertainties to consider. The small vertical antenna beam width and the low antenna heights in urban areas lead to many propagation paths and simply taking the antenna pattern in the direction of the mobile station for computing the path loss might give incorrect results. Therefore, we apply the received power for the correlation analysis instead of a likely more erroneous path loss and compute the correlation coefficient ρ of the received power from two cells i and j by

$$\rho(i, j) = \frac{E\{P_{la}(i) \cdot P_{la}(j)\} - E\{P_{la}(i)\} \cdot E\{P_{la}(j)\}}{\sigma_p(i) \cdot \sigma_p(j)} \quad (2)$$

with

- P_{la} The local power average
- $E\{P_{la}\}$ The mean of P_{la} within a route interval
- σ_p Standard deviation of P_{la} in the route interval

The correlation coefficient ρ is computed within a route interval of 40m length and the rule (1) is applied again: $\rho(i, j)$ is only regarded as reliable if the local power average P_{la} of both cells i and j fulfil condition (1) in a 40m correlation interval.

Figure 2 shows an example for P_{la} over the travelled distance within a route interval of 40m for two cells located at the same site. Even the visual impression clearly shows the high correlation which is confirmed by the numeric result of $\rho = 0.91$. We generated many of such figures for randomly selected pairs of cells to check if the above described post-process provides plausible results.

Basically, the correlation factor ρ describes the linear dependency of P_{la} . If P_{la} from two cells is non-linear correlated ρ tends towards zero although a correlation exists. Hence, an additional check would be required to proof if a correlation can be excluded with a specific probability. This is not done within this study.

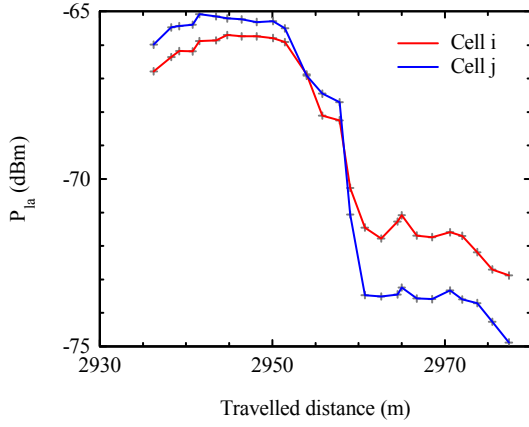


Figure 2: The local average P_{la} from two co-located cells for a short section of a route. Each '+' sign represents one value for P_{la} .

IV. RESULTS FROM THE MEASUREMENTS

Several dependencies of the slow fading correlation could be investigated. One is the dependency on the angle between the links to the regarded base station (=AAD in [1]). In agreement with other studies we did not obtain such a dependency. Typically, the network topology in larger cities is close to a regular grid. Thus, if the AAD is small the corresponding sites are widely separated and a quite large part of both radio paths is not common [3] [5]. This leads very likely to different shadowing processes on both radio paths and, consequently, to low correlated slow fading even for small AAD. Therefore, we do not further regard the AAD dependency of the slow fading correlation.

A more promising aspect is to differ between two cases: The involved cells are located 1) at the same site or 2) at different sites. Thus, we divide the computed correlation coefficients ρ in

- ρ_{ds} Cells are located at different sites
- ρ_{co} Both cells are co-located at the same site

The evaluation procedure described in the previous chapter supplies per 40m route interval at least one correlation

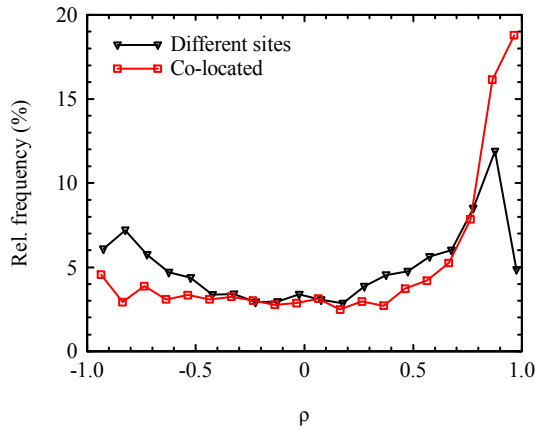


Figure 3: The relative frequency of the correlation coefficient ρ obtained in the northern part of Cologne city centre.

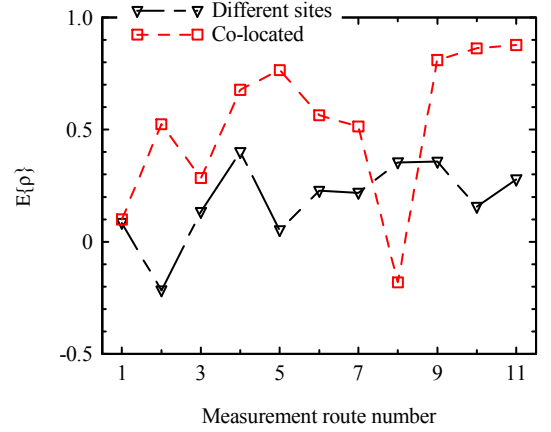


Figure 4: The mean $E\{\rho\}$ of the correlation coefficient ρ for the different measurement routes. The route numbering is given in Table 1.

coefficient. If more than two cells in a route interval fulfil the criteria (1) we even get two or more correlation coefficients per 40m route interval. Due to the overall measured route of around 100km this procedure provides a large number of correlation coefficients which are statistically evaluated for the individual measurement areas or cities (see Table 1). This individual handling enables to compare the various correlation coefficient distributions and to determine those which might be regarded as typical.

A distribution of the correlation coefficient which is typical for Cologne city centre is given in Figure 3. As expected, large correlation coefficients occur much more frequently for cells at the same site than for cells at different sites. But, even for cells at different sites we get from Figure 3 a probability of 15% for $\rho_{ds} > 0.8$.

In order to compare the correlation coefficients of the various measurement routes their mean values are given in Figure 4. The route numbering is given in Table 1. Routes no. 1 – 3 are going along straight and wide streets in Cologne where almost everywhere LOS to the serving site is given. It's interesting to see that ρ_{co} is quite low for those LOS routes since for LOS we would expect high correlated slow fading as observed in [5]. However, the sites are located on roof tops

No.	Route/Area	Part of ρ -values	Location
1	LOS	0.7 %	Cologne
2	LOS	0.7 %	
3	LOS	0.6 %	
4	Residential area	3.5 %	Cologne
5	Ring around centre	3.2 %	Cologne City Centre
6	Northern part	7.0 %	
7	Middle part	5.8 %	
8	Southern part	3.7 %	Cologne City Centre
9	Friedrichshafen	6.3 %	
10	Leeuwarden	43.5 %	
11	Drachten	24.6 %	Netherlands

Table 1: The route numbering used in Figure 4. The 3rd column contains the part of the correlation coefficients (=rho-values) computed per measurement route. The total number is 85200. No. 1-3 are long, wide and straight streets where mainly LOS is given.

along those streets and measurements in the intra-site inter-sector transition regions are only available directly under the base station antennas where even the local power average P_{la} fluctuates extremely. Thus, we do not regard this result as typical for LOS.

But also the other measurements areas in Cologne (routes No. 4-8 in Figure 4) have low values for ρ_{co} . As a threshold, signals with $\rho \leq 0.7$ are generally considered to be uncorrelated [4]. Since ρ_{co} is close to or even below 0.7 for the routes No. 4-8 means that even the signal coming from cells of the same site would not be correlated. This might be caused by more extensive multi-path propagation in dense urban area if the base station antennas are only few metres above the surrounding roof-tops and highly focussing antennas are used. This assumption is further verified by much larger ρ_{co} for all other cities (No. 9-10 in Figure 4) which are much smaller than Cologne and, thus, have not such large high-density areas as Cologne city centre. According to the means of ρ_{ds} in Figure 4 the slow fading from cells of different sites is clearly uncorrelated for all measurement routes.

The distributions of ρ_{co} obtained from both cities in the Netherlands in Figure 5 indicate a better correlation of the signals from co-located cells as observed from Cologne. A very similar distribution is also given for Friedrichshafen. Therefore, a distribution as in Figure 5 might be regarded as typical for median-sized cities having less dense urban areas as large cities like Cologne.

Since the measurements performed in the Netherlands have a higher sample rate the statistic evaluation has to be done separately for the cities in Germany and the Netherlands. For all measurements in Germany the probability for $\rho_{co} > 0.7$ is 43% and for the Netherlands it is 67%. As mentioned, the slow fading correlation differs due to different urban environment since the measurements in Germany are clearly dominated from those in Cologne city centre (see 3rd column in Table 1) which is regarded as a very dense urban area.

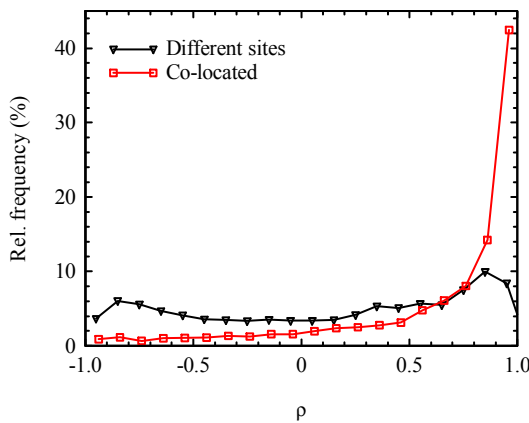


Figure 5: The relative frequency of the correlation coefficient ρ obtained from all measurements in the Netherlands. Please note that only medium-sized cities are regarded. Each marker represents one ρ -interval.

V. IMPACT ON THE PREDICTION

The major input for the throughput prediction in radio network planning tools is the SINR. Regarding HSDPA the SINR is given by

$$SINR = \frac{P_{T,HS}(i)a(i)}{(1-\alpha)P_T(i)a(i) + \sum_{\substack{j=1 \\ j \neq i}}^{N_{cell}} P_T(j)a(j) + N_{th}} \quad (3)$$

with

$P_{T,HS}$	HSDPA Transmission power
P_T	Predicted total transmission power per cell
a	Path loss
i	Index of the serving cell
N_{Th}	Thermal noise power
α	Orthogonality factor
N_{cell}	Number of cells taken into account

In radio network planning the higher quantiles, e.g. 90%, are of interest. A 90% quantile means that the predicted value is exceeded with a probability of 90%. Thus, the parameters of the SINR distribution have to be computed and for this purpose we reform (3) to

$$SINR = \frac{P_{T,HS}(i) / P_T(i)}{(1-\alpha) + \sum_{\substack{j=1 \\ j \neq i}}^{N_{cell}} \frac{P_T(j) \cdot a(j)}{P_T(i) \cdot a(i)} + \frac{N_{th}}{P_T(i) \cdot a(i)}} \quad (4)$$

In the RF planning tool PegaPlan [8] the SINR distribution is computed with an analytical approach [7]. If we express the ratio in the denominator in logarithmic units we get a sum of two normal distributed values resulting in a normal distribution again with a variance of [2]

$$\sigma_{quot}^2 = 2 \cdot \sigma_{sf}^2 \cdot (1-\rho) \quad (5)$$

where ρ represents the correlation factor and σ_{sf} the

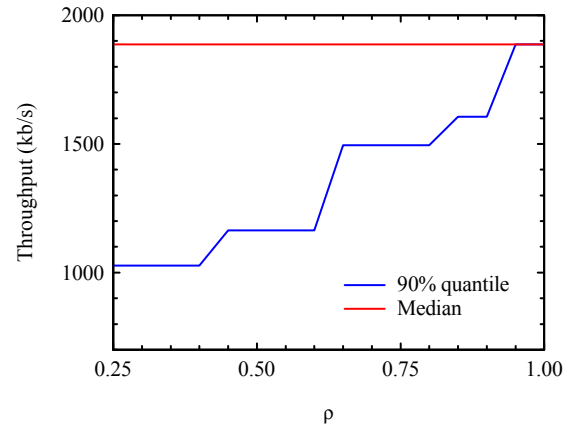


Figure 6: The impact of the correlation coefficient ρ on the computed HSDPA throughput. The step-wise graph is coming from assigning the SINR to integer CQI. One interfering cell is assumed and its level is 1dB below the power of the serving cell. The slow fading standard deviation = 4dB. 90% quantile: Throughput which is exceeded with 90% probability.

standard deviation of the slow fading. In this step of the calculation we check if the interfering cell j is located at the same site as the serving cell i and, if this is true, we apply the correlation factor ρ_{co} . The sum itself represents a sum of log-normal distributed values which gives a log-normal distributed again. The sum has to be computed in linear units which requires to transform mean and variance from linear units to logarithmic units and back again [6]. Please note that the random property of the cell transmission power P_T has to be taken into account [7]. A similar approach is implemented in PegaPlan for LTE too.

Figure 6 demonstrates how the slow fading correlation affects the 90% throughput quantile. The power of the interfering cell is assumed as 1dB below the serving cell power and $\sigma_{sf} = 4$ dB is assumed. From the uncorrelated case ($\rho = 0.25$) to the correlated case ($\rho > 0.7$) the throughput increases by 50%.

Finally, the impact of a higher correlation on the predicted HSDPA throughput is shown in Figure 7. As reference serves a prediction with a unique value for the correlation coefficient $\rho_{co} = \rho_{ds} = 0.25$ in Figure 7.a. Applying $\rho_{co} = 0.75$ in Figure 7.b increases the throughput in the transition region between co-located cells. The predicted throughput is now closer to our experience from throughput measurements. However, this significant increase of the throughput is only given if a co-located cell is the dominant interfering cell. But even if stronger interfering cells from other sites are involved too the higher value for ρ_{co} might increase the predicted throughput. Therefore, to differ between inter- and intra-site slow fading correlation improves the precision of the downlink prediction.

VI. CONCLUSION

In order to further improve the cell edge throughput prediction the slow fading correlation properties of signals from different cells are analysed. A measurement system of the usual drive test equipment is applied which enables to collect a large amount of data. A suited post-process procedure is proposed and verified.

Measurements from the Deutsche Telekom's UMTS network in four cities of different sizes in Germany and the Netherlands are evaluated. Over-all, the measured route is on the order of 100km and around 150 cells are involved. Typically, the base station antennas are located few meters above the surrounding roof tops and the sites are equipped with 3 sectors.

All measurements clearly show that the slow fading of signals from cells located at different sites is uncorrelated. Furthermore, we did not obtain a relation between the slow fading correlation and the angle between the links to the regarded cells. A significant higher correlation is observed for signals from cells of the same site. In medium-sized cities with less dense urban area more than 60% of the correlation coefficients are above 0.7. In the very dense urban area of Cologne city centre the correlation is slightly lower and around 45% of the correlation coefficients are greater than 0.7.

The different correlation properties have been implemented in the RF planning tool PegaPlan. With a higher

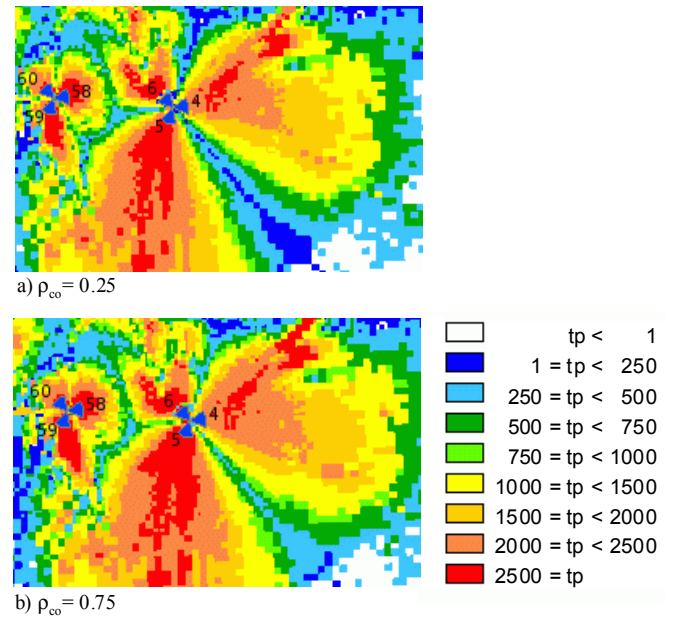


Figure 7: The predicted 90% quantile of the HSDPA throughput ($=tp$; in Mb/s) for two slow fading correlation coefficients ρ_{co} of co-located cells. The blue circle segments represent the base station antennas.

intra-site correlation of the slow fading the predicted HSDPA throughput in the transition region between cells of the same site is significantly increased. The predicted throughput is now closer to the measured throughput in such areas. Therefore, to apply different correlation coefficients for intra- and for inter-site slow fading improves the cell edge prediction in the downlink in particular for single frequency networks like UMTS and LTE.

REFERENCES

- [1] V. Graziano, 'Propagation correlations at 900MHz', IEEE trans. on Veh. Tech., Vol. 27, pp. 182 – 189, Nov. 1978
- [2] S. Saunders and B. Evans, 'The spatial correlation of shadow fading in macrocellular mobile radio systems', IEE Coll. on Prop. Aspects of Fut. Mob. Sys., London, Oct. 1996, pp. 2/1–2/6.
- [3] N. Jalden et al, 'Inter- and Intra-site correlations of large-scale parameters from macrocellular measurements at 1800 MHz', EURASIP J. Wireless Comm. and Networking, vol. 2007, No. 3, August 2007
- [4] J. Weitzen, T.J. Lowe, 'Measurement of angular and distance correlation properties of Log-Normal shadowing at 1900MHz and its application to design of PCS systems', IEEE Trans. on Veh. Tech., Vol. 51, No. 2, March 2002, pp. 265 – 273
- [5] S: Jäckel et. al, 'Intercell interference measured in urban areas', Proc. IEEE International Conference on Communications, Dresden, June 2008
- [6] David Parsons, The Mobil Radio Propagation Channel, Pentech Press Publishers, London 1992
- [7] B. Schröder et al., 'An analytical approach for determining coverage probabilities in large UMTS networks'. Proc. of IEEE VTC Fall, Atlantic City, USA, Oct. 2001
- [8] PegaPlan web site: <http://www.pegaware.com>